cis- and *trans*-Dimolybdenum(II) Complexes with Asymmetrically 2,7-Disubstituted Naphthyridines as Bridging Ligands

Markus Mintert and William S. Sheldrick*

Lehrstuhl für Analytische Chemie, Ruhr-Universität Bochum, D-44780 Bochum

Received January 24, 1996

Key Words: Dimolybdenum(II) complexes / Substituted naphthyridines

Treatment of $[Mo(CO)_6]$ with Hmamnp (2-acetamido-7-methyl-1,8-naphthyridine) in diglyme at 100°C affords the mononuclear complex $[Mo(CO)_4(Hmamnp)]$ **1**, an intermediate product on the reaction pathway to tetrasubstituted species of the type $[Mo_2L_4]$. A disubstituted intermediate product *cis*-$[Mo_2(mphamnp)_2(OAc)_2]$ **2** (Hmphamnp) (2-acetamido-5-methyl-7-phenyl-1,8-naphthyridine) may be isolated from the reaction of $[Mo_2(OAc)_4]$ with $mphamnp^-$ in THF. The relative stabilisation of such products is a result of the steric demands of the coplanar 2-acetamido substituents. **2** and the tetrasubstituted complexes *trans*-$[Mo_2(mbznnp)_4]$ **3** (Hmbznnp = 2-benzylamino-7-methyl-1,8-naphthyridine), *cis*-$[Mo_2(mphonp)_4]$ **4**, and *trans*-$[Mo_2(mphonp)_4]$ **5** (Hmphonp = 5-methyl-7-phenyl-1,8-naphthyridin-2-one) all exhibit the electronically prefered μ-N^1,X^2 bridging mode. Steric effects are responsible for the isolation of the unusual *cis* isomer **4**.

Although 1,8-naphthyridine (np) has been shown to be capable of bridging metal–metal bonds in the dinuclear complexes $[Ni_2Br_2(\mu\text{-np})_4]BPh_4$[1] and $[Rh_2(\mu\text{-np})_4]Cl_4$[2], it has typically been found to act as a mono- or bidentate ligand in mononuclear complexes such as $[CuCl_2(np)_2]$, $[PtCl(np)(PEt_3)_2]BF_4$, $[Cd(np)_4](ClO_4)_2$ and $[Fe(np)_4](ClO_4)_2$[3–6]. However, in recent years a number of compounds containing dinucleating symmetrically 2,7-disubstituted 1,8-naphthyridines have been reported. The crescent-shaped ligand dpnp [2,7-bis(2-pyridyl)-1,8-naphthyridine] has been employed in the preparation of dinuclear complexes of the type $[M_2(OAc)_3(\mu\text{-dpnp})]PF_6$ (M = Ru, Rh)[7,8], which contain M_2^{4+} cores and axially coordinating dpnp pyridine rings. Both the above Ru(II,II) complex and the structurally analogous Ru(II,III) species $[Ru_2(OAc)_3(\mu\text{-dcnp})]$ (dcnp = 1,8-naphthyridin-2,7-dicarboxylate)[9] were characterised by X-ray crystallography. A tetranuclear complex $[\{Mo_2(O_2C\text{-}t\text{-}Bu)_3\}_2(\mu\text{-donp})] \cdot 2$ thf (H_2donp = 1,8-naphthyridin-2,7-dione), containing two discrete Mo–Mo quadruple bonds of length 2.10 Å, in close proximity at a central Mo–Mo distance of 3.17 Å, has been recently studied by Chisholm and co-workers as a molecular model for subunits of stiff-chain polymers[10].

Scheme 1. 2,7-disubstituted naphthyridines

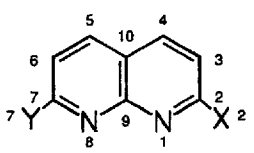

We have recently demonstrated that asymmetrically 2,7-disubstituted 1,8-naphthyridines L containing potential donor atoms as 2-substituents can be used to prepare dinuclear complexes of the type $[M_2L_4]$ for M = Mo(II), Ru(II) and Rh(II). Four anionic ligands (Hmonp = 7-methyl-1,8-naphthyridin-2-one, Hmsnp = 7-methyl-1,8-naphthyridin-2-thione) bridge the quadruple Mo–Mo bonds in *trans*-$[Mo_2(monp)_4]$ and *trans*-$[Mo_2(msnp)_4]$ and exhibit analogous N^1,X^2 (X = O, S) coordination modes[11]. In contrast N^1,N^8 coordinated naphthyridine ring systems are observed for the doubly bonded Ru_2^{4+} core in $[Ru_2(monp)_4]$. These findings prompted us to study the reation of $[Ru_2Cl(OAc)_4]$ with Hmphonp (5-methyl-7-phenyl-1,8-naphthyridin-2-one) in methanol at reflux, which leads to the successive formation of the polar complex *trans*-$[Ru_2Cl(mphonp)_2(OAc)_2]$, *trans*-$[Ru_2(mphonp)_2(OAc)_2]$, and $[Ru_2(mphonp)_4]$[12]. The reduction of the Ru_2^{5+} core in *trans*-$[Ru_2Cl(mphonp)_2(OAc)_2]$ is accompanied by a change in the coordination mode of the dinucleating $mphonp^-$ anions from N^1,O^2 to N^1,N^8 in *trans*-$[Ru_2(mphonp)_2(OAc)_2]$. Steric crowding of *cis*-sited 2- and 7-substituents leads to a renewed coordination change for one of these *trans*-sited naphthyridine derivatives in *trans*-$[Ru_2(mphonp)_2(OAc)_2]$ upon substitution of the last two briding acetate ligands. As a result the final tetrasubstituted complex $[Ru_2(mphonp)_4]$ contains three N^1,O^2 coordinated $mphonp^-$ ligands.

These fascinating results led to the present work in which we have investigated the role of electronic and steric factors in the formation of dimolybdenum(II) complexes for a series of 2,7-disubstituted naphthyridine derivatives. We chose Hmamnp (2-acetamido-7-methyl-1,8-napthyridine[13]), Hmphamnp (2-acetamido-5-methyl-7-phenyl-1,8-naphthyridine[14]), Hmbznnp (2-benzylamino-7-methyl-1,8-naphthyridine[15]) and Hmphonp (5-methyl-7-phenyl-1,8-naphthyridin-2-one[12]) so as to provide a systematic vari-

  0009–2940/96/0606–0683 $ 15.00+.25/0

Scheme 2

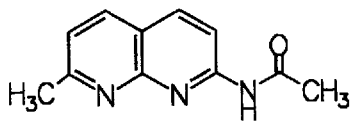

Hmamnp

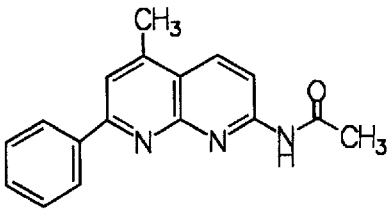

Hmphamnp

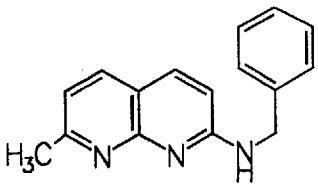

Hmbznnp

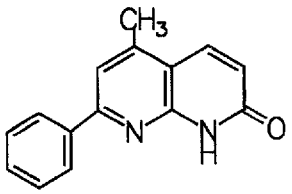

Hmphonp

Scheme 3. **1** and **2**

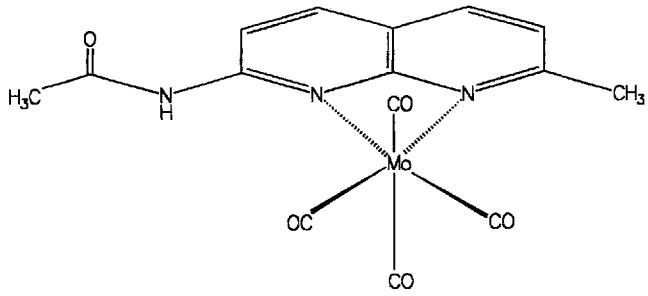

1

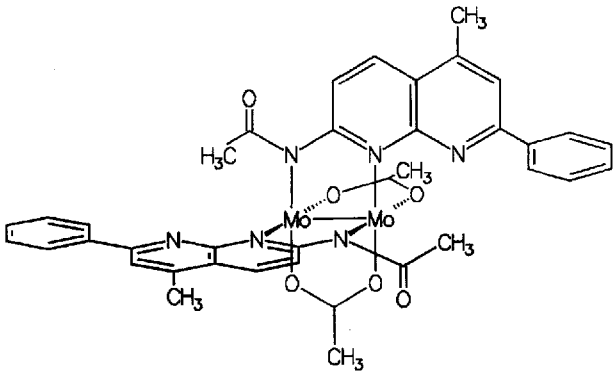

2

ation (a) in the nature of the donor atom X^2 and (b) in the bulkiness of the substituent Y^7.

Dimolybdenum(II) complexes $[Mo_2L_4]$ can typically be prepared by the reaction of $[Mo(CO)_6]$ with the dinucleating ligand HL in diglyme at 190°C or by treatment of $[Mo_2(OAc)_4]$ with L^- in THF at room temperature. During the course of the present work, we established that the former method generally provides better yields for 2-X-7-methyl substituted naphthyridines, the latter method for 2-X-7-phenyl derivatives. The increased steric demands of the presumably coplanar 2-acetamido substituents in Hmamnp and Hmphamnp lead to a relative stabilisation of intermediate products such as $[Mo(CO)_4(Hmamnp)]$ (**1**) and *cis*-$[Mo_2(mphamp)_2(OAc)_2]$ (**2**), which provides an insight into possible reaction pathways to the tetrasubstituted complexes $[Mo_2L_4]$. Analogous compounds could not be isolated for the less sterically demanding ligands Hmbznnp and Hmphonp.

Reaction of $[Mo(CO)_6]$ with Hmamnp in a 1:2 molar ratio in diglyme at 190°C leads to the formation of a product or product mixture whose very limited solubility in organic solvents prevents further characterisation. However the FAB mass spectra of the product exhibits the expected molecular ion for a dinuclear complex $[Mo_2(mamnp)]_4$. In contrast, the monomeric compound $[Mo(CO)_4(Hmamnp)]$ (**1**) may be isolated in good yield for a 1:1 molar ratio of the starting compounds at 100°C. The structure of one of the two independent molecules in the asymmetric unit of **1** is depicted in Figure 1. The κ^2N^1,N^8 coordination mode in **1** leads to a narrow N(11)–Mo(1)–N(18) bite angle of 58.5(2)° and wide Mo(1)–N(11)–C(12) and Mo(1)–N(18)–C(17) angles of 145.8(6) and 148.0(6)°. As expected a pronounced shortening is observed for the Mo–C bonds [1.936(9), 1.946(9) Å] *trans* to the weak Mo–N(naphthyridine) bonds [2.276(6), 2.314(7) Å]. This *trans* influence is also apparent in the IR spectrum of **1**, which exhibits two strong CO bands at 2012 [C(11′)–O(11′)/C(12′)–O(12′)] and 1975 cm^{-1} [C(13′)–O(13′)/C(14′)–O(14′)]. The amide methyl group adopts the sterically favourable *trans* position to the $C^2–N^2$ bond in both independent molecules. The isolation of **1** indicates that the first step in the reaction between $[Mo(CO)_6]$ and 2-substituted naphthyridines HL will lead to the formation of a mononuclear Mo(0) complex $[Mo(CO)_4HL]$. As the present work establishes an unequivocal preference for the bridging μ-1κN^1:2κX^2 mode in Mo(II,II) complexes it may be assumed that the subsequent ligand substitution, oxidation and dimerisation required for the

formation of $[Mo_2L_4]$ will be accompanied by the necessary coordination shift from N^1,N^8 to X^2,N^1.

Figure 1. Structure of the first independent molecule of $[Mo(CO)_4(Hmamnp)]$ **1**. Selected bond lengths (Å) and angles (°): Mo(1)–N(11) 2.276(6), Mo(1)–N(18) 2.314(7), Mo(1)–C(11′) 2.042(8), Mo(1)–C(12′) 2.042(8), Mo(1)–C(13′) 1.936(9), Mo(1)–C(14′) 1.946(9); N(11)–Mo(1)–N(18) 58.5(2), C(13′)–Mo(1)–N(11) 107.0(3), C(14′)–Mo(1)–N(18) 106.0(3), C(13′)–Mo(1)–C(14′) 88.5(4)

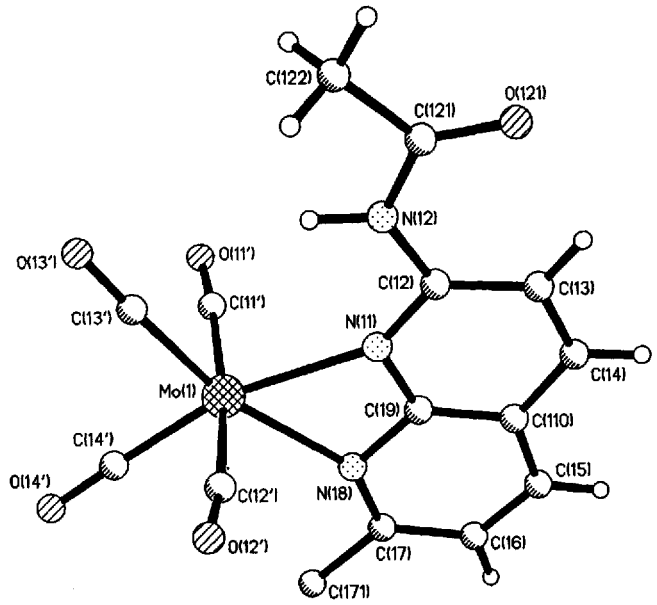

The mixed ligand dinuclear complex *cis*-$[Mo_2(mphamnp)_2(OAc)_2]$ also provides an example of a kinetically stabilised intermediate product, in the case on the reaction pathway between $[Mo_2(OAc)_4]$ and 2-substituted naphthyridine anions L^- in thf. Although FAB mass spectroscopy confirms that $[Mo_2(mphamnp)_4]$ is indeed produced by the reaction of $[Mo_2(OAc)_4]$ and Hmphamnp in 1:4 molar ratio in the presence of *n*-BuLi in THF, it also confirms the presence of a significant contamination through the partially substituted products *cis*-$[Mo_2(mphamnp)_2(OAc)_2]$ and $[Mo_2(mphamnp)_3(OAc)]$. Separation by fractonal crystallisation or liquid chromatography proved to be unsuccessful. However **2** (Figure 2) may be obtained as the only product by treatment of $[Mo_2(OAc)_4]$ with $mphamnp^-$ in a 1:2 molar ratio in thf at room temperature. The 2-substituted napthyridine ligands adopt the briding μ-1κN^1:2κN^2 mode and are sited *cis* to one another in a head to tail arrangement. **2** exhibits C_2 symmetry both in the crystal lattice and in solution with the consequence that only one set of resonances is recorded for the naphthyridine protons in the ^{1}H-NMR spectrum ($CDCl_3$). In contrast to **1**, for which the 2-acetamido substituent and the aromatic naphthyridine skeleton are effectively coplanar, **2** exhibits a pronounced degree of relative twisting. This is necessary in order to lengthen non-bonded contacts between adjacent 2-acetamido and 7-phenyl substituents as evidenced by the C(22)···C(72a) distance of 3.53 Å. The interplanar angle of 30.44° between the amide and naphthyridine planes in **2** leads to a reduction in the partial double bond character of N(2)–C(21), which lengthens from 1.39(1) Å in **1** to 1.43(2) Å. The Mo–Mo distance in **2** [2.097(2) Å] is similar to that of 2.093(1) in $[Mo_2(OAc)_4]$[16] but markedly longer than the value of 2.037(3) Å obtained for the comparable tetrasubstituted complex *trans*-$[Mo_2(amnpy)_4]$[17] (Hamnpy = 2-acetamidopyridine). Both of the dinucleating ligands display relatively wide "bites" as evidenced by the N(1)···N(2) and O(11)···O(12) distances of 2.35 and 2.18 Å in comparison to the Mo–Mo distance of 2.097 Å. This leads to Mo–Mo–O and Mo–Mo–N angles wider than 90° with the effect being particularly pronounced for the amide nitrogen N(2) [95.0(3)°]. The isolation of the *cis* configurated disubstituted complex **2** for $mphamnp^-$ with its sterically demanding substituents in both the 2- and 7-positions suggests that a similar reaction pathway will be adopted upon treatment of $[Mo_2(OAc)_4]$ with other (less sterically demanding) 2,7-disubstituted naphthyridine ligands such as $mphonp^-$ (products **4** and **5**). Substitution of the two remaining acetate bridging ligands in disubstituted complexes of the type *cis*-$[Mo_2L_2(OAc)_2]$ should lead to tetrasubstituted species $[Mo_2L_4]$ with either *cis*-$MoN^1_2X^2_2$ or *trans*-$MoN^1_2X^2_2$ coordination geometries. Kinetic, steric and electronic factors will be expected to influence the product ratio.

Figure 2. Structure of *cis*-$[Mo_2(mphamnp)_2(OAc)_2]$ **2**. Selected bond lengths (Å) and angles (°): Mo(1)–Mo(1a) 2.097(2), Mo(1)–N(1) 2.137(11), Mo(1)–N(2a) 2.192(10), Mo(1)–O(11) 2.131(9), Mo(1)–O(12a) 2.135(8); Mo(1a)–Mo(1)–N(1) 90.6(3), Mo(1a)–Mo(1)–N(2a) 95.0(3), Mo(1a)–Mo(1)–O(11) 92.8(3), Mo(1a)–Mo(1)–O(12a) 91.4(3), N(1)–Mo(1)–N(2a) 95.1(4), N(1)–Mo(1)–O(11) 174.4(4), N(2a)–Mo(1)–O(12a) 173.2(4)

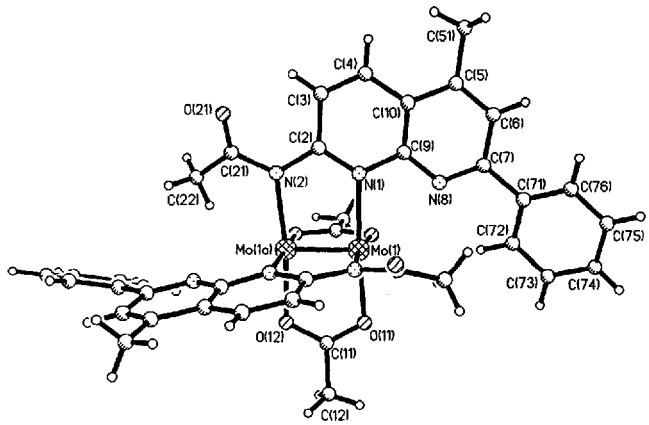

It is instructive to compare this proposed reaction pathway with that adopted for the reaction of $[Ru_2Cl(O_2CMe)_4]$ with $mphonp^-$ which contrastingly allows the isolation of an intermediate product *trans*-$[Ru_2(mphonp)_2(OAc)_2]$ with a bridging μ-1κN^1:2κN^8 mode. The *trans* configuration of this Ru(II,II) species may be assumed to be a consequence of the formation of *trans*-$[Ru_2(mphonp)_2(OAc)_2]$ from the polar Ru(II,III) complex *trans*-$[Ru_2Cl(mphonp)_2(OAc)_2]$ which necessarily contains the 2,7-disubstituted naphthyridine ligands in a head to head arrangement. As will be discussed later electronic factors are responsible for the differing N^1,X^2 and N^1,N^8 dinucleating modes in the disubstituted Mo(II,II) and Ru(II,II) complexes.

cis and *trans* Isomers for $[Mo_2L_4]$

Treatment of $[Mo(CO)_6]$ with Hmbznnp in diglyme at 190°C affords the N^1,N^2 bridged tetrasubstituted complex *trans*-$[Mo_2(mbznnp)_4]$ **3** in which the individual molybdenum atoms exhibit *trans*-$MoN^1_2X^2_2$ geometries as previously reported for $[Mo_2(monp)_4]$ and $[Mo_2(msnp)_4]$[11]. In order to minimize non-bonded contacts, the benzylamino phenyl rings orientate themselves approximately perpendicular to their own naphthyridine ring systems (Figure 3). The Mo–Mo distance of 2.091(3) Å is similar to those of $[Mo_2(OAc)_4]$, *trans*-$[Mo_2(monp)_4]$ [2.090(4) Å][11] and **2** [2.097(2) Å]. As also observed for **2** the Mo–N^2 distances [average 2.21(1) Å] are significantly longer than those to N^1 of the naphthyridine system [average 2.13(1) Å]. The relatively wide bite angle of the dinucleating ligands leads to average Mo–Mo–N^1/N^2 angles larger than 90° with this effect (as for **2**) being more pronounced for the benzylamino nitrogen atoms [average Mo–Mo–N^2 = 94.8(4)°]. Steric crowding is minimal for adjacent 2- and 7-substituents in **3** with the result that the N–Mo–No–N torsion angles at the central quadruple bond adopt values close to zero [0.2–1.3°]. The observation of only one set of ^{1}H-NMR signals for the aromatic protons in **3** indicates that the complex D_{2d} symmetry in solution.

Figure 3. Structure of *trans*-$[Mo_2(mbznnp)_4]$ **3**. Selected bond lengths (Å) and angles (°): Mo(1)–Mo(2) 2.091(3), Mo(1)–N(11) 2.20(1), Mo(1)–N(21) 2.20(1), Mo(1)–N(32) 2.13(2), Mo(1)–N(42) 2.13(2), Mo(2)–N(12) 2.14(1), Mo(2)–N(22) 2.13(1), Mo(2)–N(31) 2.21(1), Mo(2)–N(41) 2.22(1); Mo(2)–Mo(1)–N(11) 90.7(3), Mo(2)–Mo(1)–N(21) 89.4(4), Mo(1)–Mo(2)–N(31) 90.0(4), Mo(1)–Mo(2)–N(41) 91.2(4), Mo(1)–Mo(1)–N(12) 94.5(4), Mo(1)–Mo(2)–N(22) 94.7(4), Mo(2)–Mo(1)–N(32) 95.3(4), Mo(2)–Mo(1)–N(42) 94.2(4)

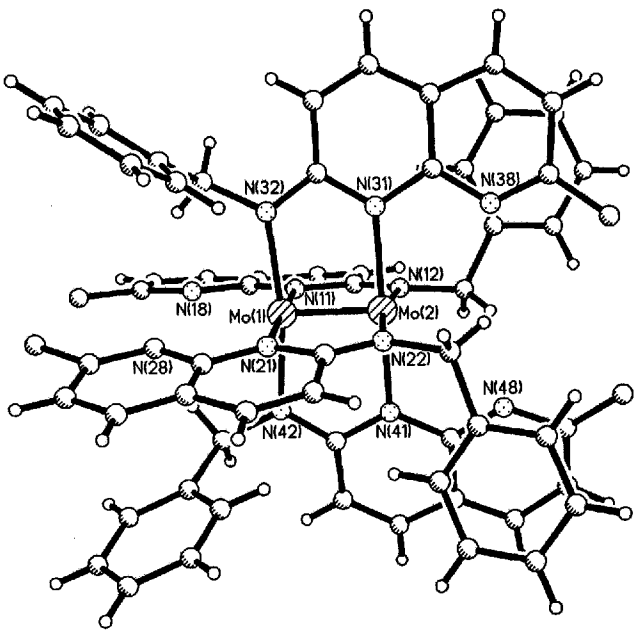

The naphthyridine derivative mphonp$^-$ with its sterically demanding 7-phenyl substituent forces three of the dinucleating ligands in $[Ru_2(mphonp)_4]$ to adopt the electronically less favourable N^1,O^2 coordination mode[12]. Individual *cis*-$RuN^1_2N^8O^2$ and *cis*-$RuN^1_2O^2_2$ geometries are exhibited by the

Scheme 4. **3**–**5**

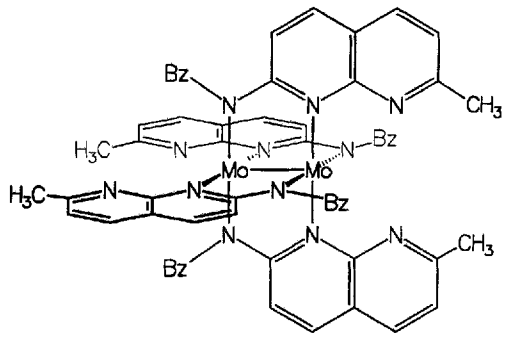

3

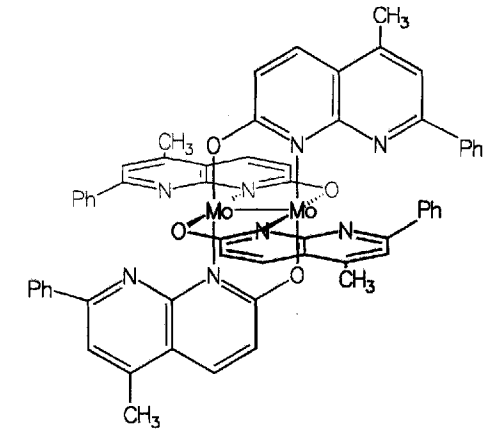

4

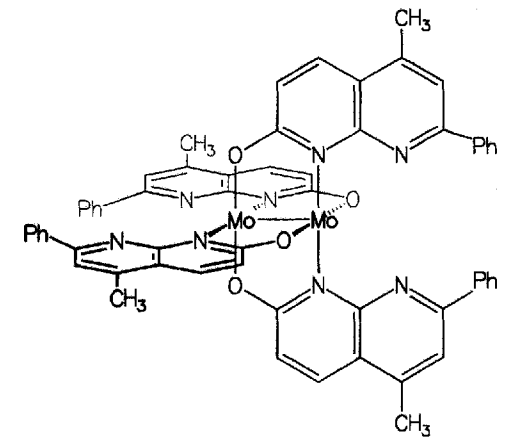

5

ruthenium atoms in this complex. Extreme steric crowding of the adjacent 7-phenyl rings also leads to a pronounced twisting of the naphthyridine ligands relative to the Ru–Ru double bond. The degree of twisting may be gauged from the N^1–Ru–Ru–N^8 torsion angle of 15.8° which is accompanied by three O^2–Ru–Ru–N^1 torsion angles in the range 18.8–22.8°. This finding prompted the question as to whether an analogous *cis*-$MoN^1_2O^2_2$ geometry will be pre-

fered instead of the typical *trans*-$MoN_2^1O_2^2$ geometry by the sterically crowded complex $[Mo_2(mphonp)_4]$, for which a similar degree of twisting will be prevented by the significantly stronger Mo–Mo quadruple bond. In fact, treatment of $[Mo_2(OAc)_4]$ with mphonp$^-$ does indeed lead to formation of the *cis* isomer **4** (Figure 4) as the major product, which can be recrystallized in 70% yield as **4** · Et_2O by diffusion of diethyl ether into an anisole solution. However crystals of the *trans* isomer **5** · $C_{10}H_{14}$ · Et_2O (Figure 5) may also be obtained in low yield (5%) by analogous gas diffusion of diethyl ether into a cymene ($C_{10}H_{14}$) solution of the raw product. *cis*-$[Mo_2(mphonp)_4]$ exhibits C_i symmetry in the solid state but the equivalence of the aromatic proton resonances in the ^{1}H-NMR spectrum of **4** in $CDCl_3$ indicates that this point symmetry is raised to C_{2h} in solution. A *cis* arrangement of asymmetrical dinucleating ligands in a complex of the type $[Mo_2L_4]$ has only previously been observed in the complex *cis*-$[Mo_2(phnpy)_4]$[18]. In contrast the molybdenum atoms in **5** exhibit typical *trans*-$MoN_2^1O_2^2$ geometries leading to a dinuclear complex with D_{2d} symmetry in solution. **4** and **5** present the first example of the isolation and structural characterisation of *cis* and *trans* isomers for a dimolybdenum(II) complex $[Mo_2L_4]$.

Figure 4. Structure of *cis*-$[Mo_2(mphonp)_4]$ **4**. Selected bond lengths (Å) and angles (°): Mo(1)–Mo(1a) 2.079(2), Mo(1)–N(11) 2.152(8), Mo(1)–N(21) 2.166(11), Mo(1)–O(12a) 2.082(7), Mo(1)–O(22a) 2.091(9); Mo(1a)–Mo(1)–N(11) 89.3(2), Mo(1a)–Mo(1)–N(21) 88.4(2), Mo(1a)–Mo(1)–O(12a) 95.3(2), Mo(1a)–Mo(1)–O(22a) 96.6(2)

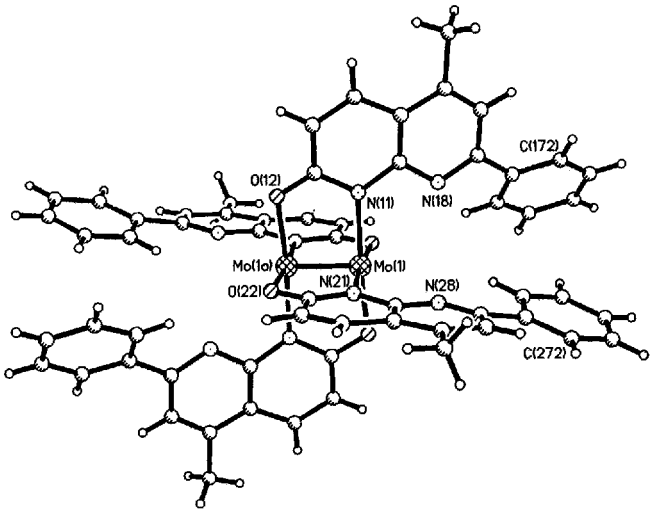

The *cis* positioned phenyl rings in **4** adopt an interplanar angle of 58.6° relative to one another and are inclined at angles of 31.5 and 15.5° to their respective naphthyridine systems. Orthogonality of the phenyl substituents would minimize their non-bonded contacts at the expense of a loss of extended π delocalisation possible for a planar naphthyridine/phenyl system. The observed molecular geometry may therefore be regarded as providing a compromise between these two goals. A surprisingly small degree of twisting about the Mo–Mo quadruple bond is indicated by the O^2–Mo–Mo–N^1 torsion angles of −3.2 and 0.9°. The crystallographic C_i symmetry also requires that *trans* sited naphthyridine systems must be coplanar. However the head to head arrangement of the *cis* sited mphonp$^-$ ligands leads these to incline their bicyclic aromatic systems away from one another at a dihedral angle of 103.7°. Relatively small O^2–Mo–Mo–N^1 torsion angles (1.5–3.8°) are also found for the *trans* isomer **5**. In this case an inclination of the *trans* sited (head to head) naphthyridine systems at respective dihedral angles of 11.8 and 10.5° enables a close to coplanar orientation of the adjacent 7-phenyl substituents (interplanar angles 11.1, 0.9°). The phenyl rings are twisted at angles of between 16.7 and 26.0° away from the planes of their respective naphthyridine systems. Similar Mo–Mo distances of 2.079(2) and 2.084(1) Å are observed for the isomers **4** and **5**. As for **2** and **3** the relatively wide bite angle of the dinucleating ligands leads to Mo–Mo–O^2 angles [average 96.0(2), 95.9(2)°] markedly wider than 90°. In contrast to **2** [90.6(3)°] and **3** [90.3(4)°] the accompanying Mo–Mo–N^1 angles in **4** and **5** are on average signficantly smaller than 90° [88.9(2), 89.2(3)°].

Our present findings confirm the electronic preference of the Mo_2^{4+} core for the N^1,X^2 rather than the alternative N^1,N^8 bridging mode by 2-substituted naphthyridines. This is the case for X^2 = O ($[\{Mo_2(O_2C\text{-}t\text{-}Bu)_3\}_2(\mu\text{-donp})]$[10], $[Mo_2(monp)_4]$[11], *cis*- and *trans*-$[Mo_2(mphonp)_4]$), X^2 = S ($[Mo_2(msnp)_4]$[11]), X^2 = N(amido) (*cis*-$[Mo_2(mphamnp)_2(OAc)_2]$) and X^2 = N(amino) (*trans*-$[Mo_2(bznnp)_4]$). As previously discussed by Chisholm et al.[10], this coordination pattern allows an energetically favourable interaction between the HOMO (δ) of the Mo–Mo quadruple bond and the LUMO (π*) of the naphthyridine system. In the absence of steric factors M_2^{4+} cores for the subsequent 2nd row transition metals (M = Ru, Rh, Pd) have been shown to adopt the alternative μ-1κN^1:2κN^8 bridging mode[12,19]. A clear preference for a *trans* arrangement of head to head 2-substituted naphthyridine ligands is also apparent from our findings. However steric factors can lead to the isolation of a *cis* isomer as demonstrated for **4**.

Experimental

All solvents were dried and distilled before use. Reactions were performed under argon by use of standard Schlenk techniques. FAB MS: Fisons VG Autospec with 3-nitrobenzyl alcohol as matrix. – ^{1}H NMR: Bruker AM 400. – FT-IR[20]: Perkin-Elmer 1700 and 1760 as KBr discs. – UV/Vis: Perkin-Elmer Lambda 15. λ_{max} is in nm, ε $dm^3 \cdot mol^{-1} \cdot cm^{-1}$. – Elementary analyses: Carlo Erba 1106 analyser. The naphthyridine derivatives Hmamnp[13], Hmphamnp[14], Hmbznnp[15] and Hmphonp[12] were synthesized according to literature procedures, as was $[Mo_2(OAc)_4]$[21]. The compound $[Mo(CO)_6]$ was obtained from Heraeus and used as received.

[Mo(CO)$_4$(Hmamnp)] (**1**): $[Mo(CO)_6]$ (0.026 g, 0.1 mmol) and Hmamnp (0.020 g, 0.1 mmol) were heated together at 100°C for 30 min. in 20 ml of diglyme. After a few minutes the colour of the solution changed from yellow to orange-red. 20 ml of diethyl ether was added to the cooled solution to afford **1** as an orange-brown precipitate, which was dried under vacuum. Yield 0.032 g (79%). – $C_{15}H_{11}MoN_3O_5$ (409.2): calcd. C 44.0, H 2.7, N 10.3; found C 43.7, H 2.9, N 11.4. – FAB MS: *m/z* (%): 409 (100) [M^+]. – ^{1}H NMR ($CDCl_3$): δ = 2.16 (s, 3H, CH_3C=O), 2.71 (s, 3H, 7-H),

Figure 5. Structure of *trans*-[Mo_2(mphonp)$_4$] **5**. Selected bond lengths (Å) and angles (°): Mo(1)–Mo(2) 2.084(1), Mo(1)–N(11) 2.15(1), Mo(1)–N(21) 2.12(1), Mo(1)–O(32) 2.07(1), Mo(1)–O(42) 2.09(1), Mo(2)–N(31) 2.15, Mo(2)–N(41) 2.13(1), Mo(2)–O(12) 2.05(1), Mo(2)–O(22) 2.07(1); Mo(2)–Mo(1)–N(11) 88.1(3), Mo(2)–Mo(1)–N(21) 90.2(3), Mo(2)–Mo(1)–O(32) 94.8(2), Mo(2)–Mo(1)–O(42) 96.1(2), Mo(1)–Mo(2)–N(31) 90.4(3), Mo(1)–Mo(2)–N(41) 88.1(3), Mo(1)–Mo(2)–O(12) 96.5(2), Mo(1)–Mo(2)–O(22) 96.1(2)

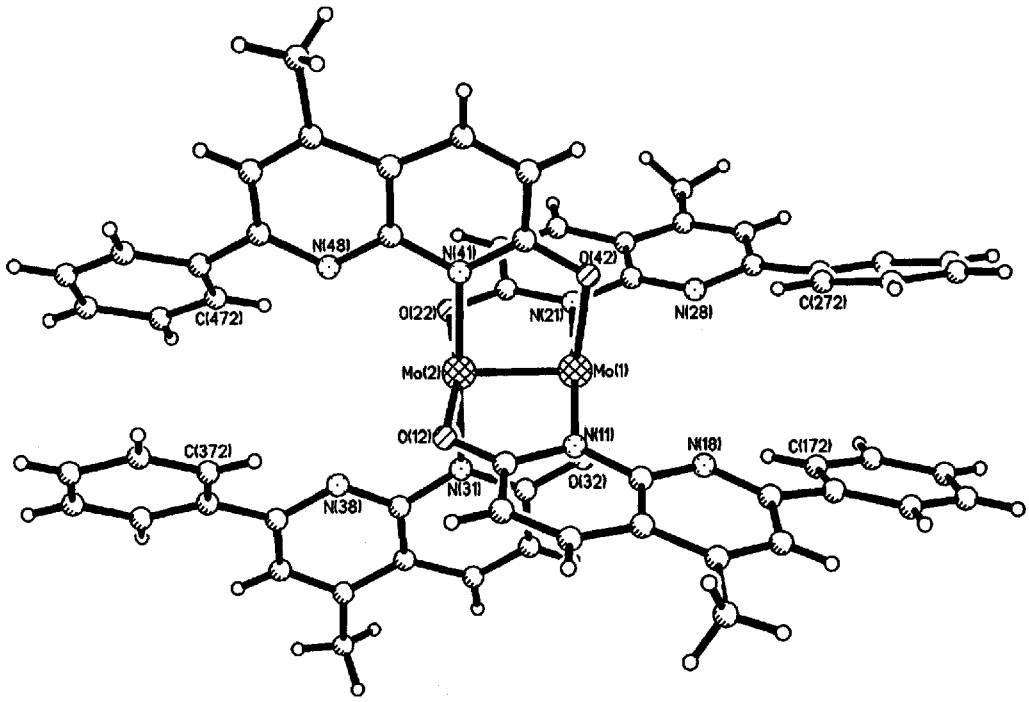

7.28 (d, 1H, 3-H), 7.88 (d, 1H, 6-H), 8.15 (d, 1H, 4-H), 8.44 (d, 1H, 5-H). – IR (KBr): $\tilde{\nu}$ = 3041 (w) (N–H), 2012 (s), 1975 (s) (C=O), 1667 (m) ($CH_3C{=}O$), 1603 (m), 1592 (s), 1312 (w), 808 (w). – UV/Vis ($CHCl_3$): λ_{max} (ε): 432 (501), 325 (1712), 289 (1683).

cis-[Mo_2(mphamnp)$_2$(OAc)$_2$] (**2**): [$Mo_2(OAc)_4$] (0.043 g, 0.1 mmol) was added to a solution of Hmphamnp (0.055 g, 0.2 mmol) and 0.2 mmol *n*-BuLi in 20 ml thf leading to a colour change from yellow to violet. After stirring for 8 h, 20 ml of pentane was added to the solution to afford **2** as a violet precipitate, which was dried under vacuum. Yield 0.071 g (83%). – $C_{38}H_{34}Mo_2N_6O_6$ (862.6): calcd. C 52.9, H 4.0, N 9.7; found C 52.4, H 4.2, N 9.1. – FAB MS: *m/z* (%): 862 (100) [M^+]. – ^{1}H NMR ($CDCl_3$): δ = 2.25 (s, 3H, $CH_3C{=}O$), 2.73 (s, 3H, 5-H), 7.33 (d, 1H, 3-H), 7.48 (m, 3H, C_6H_5), 7.73 (s, 1H, 6-H), 8.20 (m, 2H, C_6H_5), 8.53 (d, 1H, 4-H). – IR (KBr): $\tilde{\nu}$ = 1580 (s), 1511 (m), 1423 (m), 1366 (w), 1315 (m), 1252 (w), 1153 (w). – UV/Vis ($CHCl_3$): λ_{max} (ε): 566 (1881), 349 (16230), 280 (2040).

trans-[Mo_2(mbznnp)$_4$] (**3**): [$Mo(CO)_6$] (0.026 g, 0.1 mmol) and Hmbznnp (0.050 g, 0.2 mmol) were heated together at 190°C for 30 min. in 20 ml diglyme. The colour of the solution changed rapidly from yellow to blue. After the solution was cooled, 20 ml of pentane was added to afford **3** as a blue precipitate, which was dried under vacuum. Yield 0.051 g (85%). – $C_{64}H_{56}Mo_2N_{12}$ (1185.1): calcd. C 64.9, H 4.8, N 14.2; found C 63.4, H 5.0, N 13.9. – FAB MS: *m/z* (%): 1186 (100) [M + H]$^+$, 937 (15) [M – mbznnp]$^+$, 593 (13) [M – Mo – 2 mbznnp]$^+$. – ^{1}H NMR ($CDCl_3$): δ = 2.62 (s, 3H, CH_3), 4.75 (d, 2H, CH_2), 6.72 (d, 1H, 3-H), 7.09 (d, 1H, 6-H), 7.34 (m, 5H, C_6H_5), 7.72 (d, 1H, 4-H), 7.81 (d, 1H, 5-H). – IR (KBr): $\tilde{\nu}$ = 2922 (w), 1701 (m), 1610 (m), 1596 (s), 1511 (s), 1397 (w), 1313 (s), 1283 (m). – UV/Vis ($CHCl_3$): λ_{max} (ε): 539 (751), 474 (1028), 342 (2859).

cis-[Mo_2(mphonp)$_4$] (**4**) *and trans-[Mo_2(mphonp)$_4$]* (**5**): [$Mo_2(OAc)_4$] (0.106 g, 0.25 mmol) was added to a solution of Hmphonp (0.237 g, 1 mmol) and 1 mmol of *n*-BuLi in 25 ml of THF leading to an immediate colour change from brown to green. After 5 min. the solution exhibited a violet colour. The solution was stirred at room temperature for 12 h. Subsequent addition of 25 ml of diethyl ether led to precipitation of a mixture of **4** and **5** as a blue product. Yield 0.263 g (93%). **4** was obtained by dissolving the product in 25 ml anisole. After filtering, crystals of **4** · Et_2O were grown by slow gas diffusion of diethyl ether into the solution. The product was dried in vacuum to afford **4** in 70% yield. – $C_{60}H_{44}Mo_2N_8O_4$ (1132.9): calcd. C 63.6, H 3.9, N 9.9; found C 64.6, H 4.6, N 9.0. – FAB MS: *m/z* (%): 1133 (100) [M^+], 897 (11) [M – L]$^+$. – ^{1}H NMR ($CDCl_3$): δ = 2.61 (s, 3H, CH_3), 6.66 (d, 1H, 3-H), 7.45 (s, 1H, 6-H), 7.51 (m, 3H, C_6H_5), 7.91 (d, 1H, 4-H), 8.03 (m, 2H, C_6H_5). – IR (KBr): $\tilde{\nu}$ = 3057 (w), 1657 (m), 1577 (s), 1537 (m), 1434 (s), 1378 (m), 1353 (m), 1108 (w), 770 (w), 692 (w). – UV/Vis (C_6H_6): λ_{max} (ε): 553 (1748), 347 (14801). Crystals of **5** · $C_{10}H_{14}$ · Et_2O were obtained in very low yield (5%) by dissolving the raw product in *p*-cymene followed by slow gas diffusion of diethyl ether into the solution.

X-ray Structural Analyses: Siemens P4 diffractometer, graphite monochromator, MoK_α radiation (λ = 0.71073 Å), SHELXTL PLUS programs[22] and SHELXL[23] (for **5**) for structure solution by direct methods and refinement by full-matrix least-squares. Semi-empirical absorption corrections were applied to the intensity data by use of ψ-scans. Hydrogen atoms were included at geometrically calculated positions for all non-solvent molecules in **1**–**5**[24]. – **1**: $C_{15}H_{11}MoN_3O_5$, M = 409, monoclinic, space group $P2_1/c$, a = 12.534(3), b = 19.673(4), c = 13.500(3) Å, β = 100.44(3)°, V = 3274(1) Å^3, Z = 8, D_{calc} = 1.660 g · cm^{-3}, μ = 8.31 cm^{-1}. Crystal

size 0.68 · 0.36 · 0.16 mm; ω-scan: $2\Theta \leq 50°$ ($0 \leq h \leq 12$, $0 \leq k \leq 23$, $-16 \leq l \leq 15$), 5937 reflections collected, 5356 symmetry-independent reflections ($R_{int} = 0.018$); max./min. transmission: 0.259/0.221; 456 parameters refined; $w^{-1} = \sigma^2(F_o) + 0.0002\ F_o^2$, $R = 0.055$, $R_w = 0.055$ for 3073 reflections with $F_o^2 > 2\sigma(F_o^2)$; largest difference peak: 0.56 eÅ^{-3}. Anisotropic temperature factors for all nonhydrogen atoms. – **2** · C_5H_{12}: $C_{43}H_{46}Mo_2N_6O_6$, $M = 935$, monoclinic space group $C2/c$, $a = 11.824(2)$, $b = 24.743(5)$, $c = 16.105(3)$ Å, $\beta = 96.99(3)°$, $V = 4677(1)$ Å^3, $Z = 4$, $D_{calc} = 1.328$ g · cm^{-3}, $\mu = 5.85$ cm^{-1}. Crystal size 0.68 · 0.08 · 0.04 mm; ω-scan: $2\Theta \leq 45°$ ($0 \leq h \leq 12$, $0 \leq k \leq 26$, $-17 \leq l \leq 17$), 3289 reflections collected, 3030 symmetry-independent reflections ($R_{int} = 0.039$); max./min. transmission: 0.378/0.339; 243 parameters refined; $w^{-1} = \sigma^2(F_o) + 0.0005\ F_o^2$, $R = 0.060$, $R_w = 0.060$ for 1569 reflections with $F_o^2 > 2\sigma(F_o^2)$; largest difference peak: 0.56 eÅ^{-3}. Anisotropic temperature factors for all nonhydrogen atoms with the exception of the *n*-pentane carbon atoms. – **3**: $C_{64}H_{56}Mo_2N_{12}$, $M = 1185$, monoclinic, space group $P2_1/c$, $a = 14.356(3)$, $b = 23.234(5)$, $c = 17.679(4)$ Å, $\beta = 107.53(3)°$, $V = 5623(2)$ Å^3, $Z = 4$, $D_{calc} = 1.400$ g · cm^{-3}, $\mu = 4.98$ cm^{-1}. Crystal size 0.42 · 0.38 · 0.30 mm; ω-scan: $2\Theta \leq 45°$ ($0 \leq h \leq 15$, $0 \leq k \leq 24$, $-18 \leq l \leq 18$), 7746 reflections collected, 7185 symmetry-independent reflections ($R_{int} = 0.074$); max./min. transmission: 0.294/0.246; 624 parameters refined, $w^{-1} = \sigma^2(F_o) + 0.0005\ F_o^2$, $R = 0.086$, $R_w = 0.083$ for 3272 reflections with $F_o^2 > 2\sigma(F_o^2)$; largest difference peak: 1.03 eÅ^{-3}. Anistropic temperature factors for the nonhydrogen atoms. – **4** · $(C_2H_5)_2O$: $C_{64}H_{54}Mo_2N_8O_5$, $M = 1207$, monoclinic space group $C2/c$, $a = 23.037(6)$, $b = 23.670(8)$, $c = 11.585(5)$ Å, $\beta = 110.86(7)°$, $V = 5903(12)$ Å^3, $Z = 4$, $D_{calc} = 1.358$ g · cm^{-3}, $\mu = 4.80$ cm^{-1}. Crystal size 0.62 · 0.48 · 0.22 mm; ω-scan: $2\Theta \leq 45°$ ($-24 \leq h \leq 23$, $-25 \leq k \leq 0$, $0 \leq l \leq 12$), 4130 reflections ($R_{int} = 0.048$); max./min. transmission: 0.435/0.364; 365 parameters refined; $w^{-1} = \sigma^2(F_o) + 0.0004\ F_o^2$, $R = 0.065$, $R_w = 0.065$ for 2276 reflections with $F_o^2 > 2\sigma(F_o^2)$; largest difference peak: 0.73 eÅ^{-3}. Anisotropic temperature factors for all nonhydrogen atoms with the exception of the diethyl ether molecule which is severely disordered. – **5** · $C_{10}H_{14}$ · $(C_2H_5)_2O$: $C_{74}H_{68}Mo_2N_8O_5$, $M = 1341$, monoclinic space group $P2_1/c$, $a = 9.371(2)$, $b = 34.293(7)$, $c = 19.434(4)$ Å, $\beta = 90.97(3)°$, $V = 6244(2)$ Å^3, $Z = 4$, $D_{calc} = 1.427$ g · cm^{-3}, $\mu = 4.62$ cm^{-1}. Crystal size 0.70 · 0.46 · 0.04 mm; ω-scan: $2\Theta \leq 45°$ ($0 \leq h \leq 11$, $0 \leq k \leq 38$, $-21 \leq l \leq 21$), 8754 reflections collected, 7970 symmetry-independent reflections ($R_{int} = 0.062$); max./min. transmission: 0.342/0.291; 696 parameters refined; $w^{-1} = [\sigma^2(F_o^2) + (0.0548 \cdot P)^2]$, $P = [\mathrm{Max}(F_o^2, 0) + 2 \cdot F_o^2]/3$; $R = 0.047$ (for 1792 reflections with $F_o^2 > 2\sigma(F_o^2)$), $wR2 = 0.1660$ for all data (refinement against F_o^2 with SHELXTL), largest difference peak: 0.30 eÅ^{-3}. Anisotropic temperature factors for all nonhydrogen atoms with the exception of the *p*-cymene molecule.

[1] L. Sacconi, C. Mealli, D. Gatteschi, *Inorg. Chem.* **1974**, *13*, 1985.
[2] W. R. Tikkanen, E. Binamira-Soriaga, W. C. Kaska, P. C. Ford, *Inorg. Chem.* **1984**, *23*, 141.
[3] E. L. Enwall, K. Emerson, *Acta Crystallogr., Sect. B* **1979**, *35*, 2562.
[4] G. W. Bushnell, K. R. Dixon, M. A. Kahn, *Can. J. Chem.* **1978**, *56*, 450.
[5] J. M. Epstein, J. C. Dewan, D. L. Kepert, A. H. White, *J. Chem. Soc. Dalton Trans.* **1974**, 1949.
[6] A. Clearfield, P. Singh, *J. Chem. Soc. Chem. Commun.* **1970**, 389.
[7] E. Binamira-Soriaga, N. L. Keder, W. C. Kaska, *Inorg. Chem.* **1990**, *29*, 3167.
[8] W. R. Tikkanen, E. Binamira-Soriaga, W. C. Kaska, P. C. Ford, *Inorg. Chem.* **1983**, *22*, 1147.
[9] J.-P. Collin, A. Jouaiti, J.-P. Sauvage, W. C. Kaska, M. A. McLoughlin, N. L. Keder, W. T. A. Harrison, G. D. Stucky, *Inorg. Chem.* **1990**, *29*, 2238.
[10] R. H. Clayton, M. H. Chisholm, J. C. Huffmann, E. B. Lobkovsky, *Angew. Chem.* **1990**, *103*, 893; *J. Am. Chem. Soc.* **1991**, *113*, 8709.
[11] W. S. Sheldrick, M. Mintert, *Inorg. Chim. Acta* **1994**, *219*, 23.
[12] M. Mintert, W. S. Sheldrick, *Inorg. Chim. Acta* **1995**, *236*, 13.
[13] E. V. Brown, *J. Org. Chem.* **1965**, *30*, 1607.
[14] R. A. Henry, P. R. Hammond, *J. Heterocycl. Chem.* **1977**, *14*, 1109.
[15] M. Mintert, W. S. Sheldrick, *J. Chem. Soc. Dalton Trans* **1995**, 2663.
[16] A. Sasajpal, P. Thornton, *Polyhedron* **1988**, *7*, 2715.
[17] F. A. Cotton, W. H. Ilsley, W. Kaim, *Inorg. Chem.* **1979**, *18*, 2717.
[18] A. R. Chakravarty, F. A. Cotton, E. S. Shamshoum, *Inorg. Chem.* **1984**, *23*, 4216.
[19] M. Mintert, W. S. Sheldrick, unpublished results.
[20] M. Mintert, Dissertation, Ruhr-Universität Bochum, **1995**.
[21] G. Holske, H. Schäfer, *Z. Anorg. Allg. Chem.* **1995**, *391*, 263.
[22] SHELXTL PLUS, Siemens Analytical X-ray Instruments, Madison, Wisconsin, USA, **1991**.
[23] G. M. Sheldrick, SHELXL-93, a program for structure refinement, Göttingen, Germany, **1993**.
[24] Further details of the crystal structure investigations are available on request from Fachinformationszentrum Karlsruhe, Gesellschaft für wissenschaftlich-technische Information mbH, D-76344 Eggenstein-Leopoldshafen, Germany, on quoting the depository numbers CSD-404794–404798.

[96019]